Ocean Engineering 284 (2023) 115451

Contents lists available at ScienceDirect

Ocean Engineering

journal homepage: www.elsevier.com/locate/oceaneng

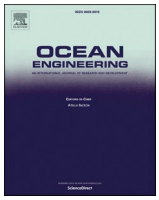

The impact of climate change on the wave energy resource potential of the Atlantic Coast of Iberian Peninsula

Ajab Gul Majidi [a,b,*], Victor Ramos [a,b], Gianmaria Giannini [a,b], Paulo Rosa Santos [a,b], Luciana das Neves [a,b,c], Francisco Taveira-Pinto [a,b]

[a] Department of Civil Engineering, Faculty of Engineering of the University of Porto (FEUP), Rua Dr. Roberto Frias, S/N, 4200-465, Porto, Portugal
[b] Interdisciplinary Centre of Marine and Environmental Research of the University of Porto (CIIMAR), Avenida General Norton de Matos, S/N, 4450-208, Matosinhos, Portugal
[c] IMDC—International Marine and Dredging Consultants, Van Immerseelstraat 66, 2018, Antwerp, Belgium

ARTICLE INFO

Keywords:
Climate change
Wave power
Seasonal variability
Renewable energy
RCP8.5

ABSTRACT

This study investigates the impact of climate change on the wave energy potential along the Atlantic coast of the Iberian Peninsula, a region acknowledged for its high wave energy resource. The research focuses on the annual and intra-annual variations in wave power for the high-emission RCP8.5 global warming scenario over different time frames: historical, near-future, and far-future. The results show a decreasing trend in the wave energy resource throughout the study area, with the most notable reductions observed in the northwestern region. The reduction in maximum annual power ranges from 15.1 to 7.2 kW/m. Changes in atmospheric circulation patterns and ocean surface temperature gradients induced by climate change effects could explain these results. This study also discusses the impacts of wave power projections on the design of wave energy converters and their future operation. The outcomes are of high interest to adapt the renewable energy infrastructure to a changing climate, ultimately also aiding in the strategic planning and cost-effective design of future wave energy projects.

1. Introduction

Changes in ocean waves can cause changes to natural coastal processes, which may have varying impacts on different human, economic, and environmental systems, including the prospective increase in critical coastal infrastructure at risk of erosion and/or inundation and the loss of coastal ecosystems, as well as alterations in the shipping sector and the available wave energy resource. The latter appears as a promising alternative form of renewable energy and has gained increasing attention in science and industry. However, in recent years, changes in the long-term wave climate have been revealed through the use of voluntary observing ships, satellite imagery, buoy measurements, reanalysis data, and numerical modeling (Shimura et al., 2015). As investment in ocean energy – including wave energy – increases, assessments of the possible future evolution of ocean energy resources become essential. The relationship between climate change and the weather has become increasingly apparent, particularly as extreme weather events have become more frequent and severe (Tabari, 2020). Small changes in critical climate variables can have a significant impact on the frequency and pattern of extreme events (Hersher, 2023). Hence, many countries worldwide are taking action to mitigate climate change.

The European Union member states have accepted long-term plans to make Europe the first world's climate-neutral continent by 2050 (The European Green Deal, 2020). In this context, the European Green Deal focuses on various climate-related policies (Rusu, 2022), in which the transition to renewable energy sources emerges as pivotal in addressing the challenge of climate change.

Wave energy has both advantages and disadvantages to consider when implementing it on a large scale. Wave energy is a predictable and consistent source of energy that produces no emissions or pollutants. This makes it a sustainable, low-carbon energy source that can help mitigate the negative impacts of climate change. Wave energy also has the potential to create jobs, boost economic growth, and reduce our dependence on imported fossil fuels, improving energy security (Lavaa, 2023). On the other hand, wave energy has several limitations, such as being location-specific, and limiting its use to areas near the ocean

* Corresponding author. Department of Civil Engineering, Faculty of Engineering of the University of Porto (FEUP), Rua Dr. Roberto Frias, S/N, 4200-465, Porto, Portugal.
E-mail addresses: ajabgulmajidi@gmail.com (A.G. Majidi), jvrc@fe.up.pt (V. Ramos), gianmaria@fe.up.pt (G. Giannini), pjrsantos@fe.up.pt (P. Rosa Santos), lpneves@fe.up.pt (L. das Neves), fpinto@fe.up.pt (F. Taveira-Pinto).

https://doi.org/10.1016/j.oceaneng.2023.115451
Received 25 May 2023; Received in revised form 11 July 2023; Accepted 22 July 2023
Available online 26 July 2023

(Bingölbali et al., 2021; Majidi et al., 2020a, 2020b). Additionally, the deployed wave energy converters (WECs) may have a negative impact on the marine ecosystem, disturb private and commercial vessels, create noise and be aesthetically unpleasant. Finally, wave energy harvesting is highly dependent on the wavelength, and the performance of WECs drops significantly in rough weather. Harvesting technologies still remain expensive to produce, difficult to scale, and slow to improve. In fact, only a few pilot projects have been constructed globally, requiring further research to determine their impacts and associated costs Majidi et al. (2021b), 2021a, 2020, Lavaa, 2023Lavaa, 2023). Similarly, to other marine renewables, it is still challenging and expensive to transport generated electricity over long distances.

Climate change, already demonstrating its multifaceted impacts on the environment, has influenced the frequency of phenomena such as storm surges and wind waves. A recent critical evaluation conducted by Pavlova et al. (2022) examined these impacts, specifically on the Caspian Sea. Despite observing no significant trends in storm activity, the study illuminated insights into extreme values and storm activities vis-a-vis the persistent climate change. Furthermore, this understanding of the maritime climate, inclusive of wave and storm regimes, has gained paramount importance in the design of coastal and offshore infrastructures. This factor is particularly vital for geographic entities like the Canary Islands, which heavily rely on maritime trade for sustenance and are characterized by distinct geographic features and construction challenges (Rodríguez-Martín et al., 2022).

The ramifications of climate change introduce additional uncertainties that underscore the need for assessing the wave energy resource under diverse climate change scenarios. Several reasons underpin this relevance. Primarily, understanding how climate change might influence the availability and variability of wave energy is vital for both developers and policymakers. This knowledge forms the bedrock of planning investments in wave energy projects, ensuring their successful performance and long-term viability. Moreover, comprehending the implications of climate change on the wave energy resource can unveil potential risks and opportunities about this renewable energy source. Alterations in wave patterns and intensity might lead to a shift in optimal locations for wave energy installations or even uncover previously unsuitable locations now fitting due to the evolving wave conditions. This information can be leveraged to prioritize wave energy investments, formulate incentive programs, and establish regulations that foster the sustainable growth of this promising renewable energy source (Reguero et al., 2019). As a result, comprehending the potential impact of climate change on wave energy resources becomes pivotal for informed decision-making about its future implementation. Subsequently, numerous recent studies have explored the wave energy potential in different regions under varying climate scenarios.

Based on the study conducted by (Goharnejad et al., 2021), it was found that the Persian Gulf region along the southern coasts of Iran presents good potential for wave energy exploitation. The study analyzed wave energy at six different points in the region over a timeframe of 30 years using numerical modeling and wind field data. This study revealed an ascending trend in mean annual wave power for the historical timeframe, while both climate change scenarios considered, RCP8.5 and RCP4.5, have descending trends, with the trend for RCP4.5 being milder.

(Rusu, 2019a) also evaluated the near future wave power resources in the Black Sea using a wave modeling system forced with wind fields provided by a regional climate model. The study found an increase in the mean wave power (P_w) under the RCP4.5 scenario in almost all the western parts of the Black Sea and the northeastern area, while under RCP8.5, P_w nearly doubles its value in comparison with the current scenario. This work highlights the importance of assessing the impact of climate change on the wave energy resource and provides valuable information for future planning and management of wave energy in the Black Sea region.

A recent study investigated the long-term sustainability of the wave energy resource in the northern part of the Gulf of Oman, considering the impact of climate change under the Socio-economic Pathway scenarios (SSP5-8.5). The study employed a third-generation wave model forced by a near-surface wind speed dataset from a high-resolution climate change model. The results suggest an increase in future P_w ranging from 21 to 45% under a high-emission scenario (Pourali et al., 2023).

Charles et al. (2012) investigated the evolution of offshore and coastal wave climates in the Bay of Biscay and the French Atlantic coast. They built a high spatial resolution dataset of wave conditions for three future greenhouse gas emission scenarios using dynamical downscaling. The study found a general decrease in wave heights (up to −20 cm during summer within the Bay of Biscay).

In addition to the studies mentioned earlier, several other studies (Chini et al., 2010; Lionello et al., 2008; Reeve et al., 2011; Rusu, 2019b; Sierra et al., 2017) have also aimed to assess the impact of climate change on wave resources in different regions. These studies provide insights into the potential effects of climate change on wave energy resources in various locations, highlighting patterns and trends that can inform future research and planning in the renewable energy sector.

The current study aims to fill an existing research gap by conducting a high-resolution and long-term assessment of wave energy resources in the coastal area of the Iberian Peninsula, one of the areas with the largest wave energy potential in continental Europe (Mørk et al., 2010; Silva et al., 2015). Rusu (2022) implemented a new wave modeling system in the North Atlantic Ocean and conducted simulations for two 20-year time intervals to assess wave climate and wave power (P_w) resources along the coastal environment of the Iberian Peninsula under the RCP4.5 climate change scenario. The study found that P_w values decreased from 12% to 20% on the western Iberian coast, with a seasonal variability of these values, highlighting the variability of P_w resources as an important consideration for their exploitation. Another study conducted by Ribeiro et al. (2020) assessed the potential changes in wave energy resources in the coastal region of the Iberian Peninsula under future climate change scenarios (RCP8.5) for the near future timeframe of 2026–2045. The study utilized a high-resolution regional wave model and a regional wind model to assess the wave and wind energy potential in the region. The results indicated that the combination of wave and wind energy could provide a more stable and reliable source of renewable energy, particularly during the winter months when the wind and wave climates are more favorable. Despite the existence of previous studies on the wave energy potential of the Atlantic Coast of the Iberian Peninsula, the potential impact of climate change on this renewable energy source has not been fully evaluated. This research addresses this gap by examining the effects of the RCP8.5 climate change scenario on wave power across various timeframes, providing valuable insights into the future of wave energy production in the region.

The coastal area of the Iberian Peninsula has one of the largest wave energy resources in continental Europe and, over the last years, it has attracted the interest of WEC developers such as CorPower, EcoWavePower, and WaveRoller (CorPower Ocean, 2023; Eco Wave Power, 2023; AW-Energy, 2023). Climate change could lead to changes in the wind climate, potentially impacting wave energy resources in the region. This study evaluates the changes in wave energy resources in the coastal area of the Iberian Peninsula due to changes in the wind climate, using the SWAN numerical wave model (Booij et al., 1999; "SWAN Team," 2020), forced with wind data from the global wind projection model CMIP5 (Taylor et al., 2012) under the RCP8.5 scenario (Riahi et al., 2011a). The model is calibrated and validated against 10 wave buoy measurements based on ERA5 wind and wave reanalysis (Hersbach et al., 2020) data using an unstructured mesh (SWAN + ADCIRC methodology) (Dietrich et al., 2012; Luettich et al., 1992) and GEBCO bathymetry data (Weatherall et al., 2015). The study assesses the variations of the wave resource under different timeframes which can contribute to implementing strategies to optimize energy extraction in long-term horizons. The use of numerical wave models, such as SWAN,

which can be used for both forecasting and hindcasting simulations (Li et al., 2016; Rusu, 2020; Rusu and GuedesSoares, 2014), has proven to be an effective tool in assessing the wave energy potential of the region and evaluating the potential impact of climate change on these resources (Ramos et al., 2017; Silva et al., 2018).

The potential influence of climate change on wave energy resources is a topic that requires in-depth investigation. In this study, the potential changes of the wave energy resource across the Iberian Peninsula's Atlantic coast are assessed for the high-emission RCP8.5 global warming scenario. To overcome the inherent difficulties of modeling climate change effects, the present work uses a carefully calibrated/validated wave model, accounting for several key parameters and sensitivities, to provide reliable wave power projections. In addition, several timeframes (*i.e.*, historical, near-future, and far-future periods) are assessed in detail.

2. Model implementation

For the present work, an unstructured mesh-based third-generation spectral phase-averaged wave model (SWAN), is used to compute the wave climate of the study area (Mazzolari, 2013; Amarouche et al., 2021; Hoque et al., 2020; Zijlema, 2010). This approach allows to capture of critical local physics, such as bathymetric features and coastlines while maintaining computational efficiency. Utilizing an unstructured grid enables superior congruence with coastal topography and grid resolution is duly adjusted according to the water depth. The unstructured grid system utilized in this study is composed of 114518 vertices, 220485 internal cells, 4261 boundary cells, 334975 internal faces, and 4288 boundary faces. The model forced with ERA5 reanalysis data was previously calibrated and validated using observation for 10 different locations and the results are published in (Majidi et al., 2023). For the calibration of the model variables, the wind-scaling factor and the wind drag formulations were tuned. These are known to be the most sensitive calibration parameters within the ST6 physics package of the SWAN model. The maximum grid size was 0.26°, while the minimum grid size was 0.002°. The bathymetry data utilized to create the unstructured mesh grid (Fig. 1) was obtained from the GEBCO datasets (Weatherall et al., 2015). Additionally, wind data projections under the RCP8.5 emission scenario (Riahi et al., 2011b) were used in this study for three different timeframes, 1979–1998, 2026–2045, and 2081–2100, from now on referred to as *His*, *Med,* and *End*, respectively. These datasets were produced by the Mediterranean Centre for Climate Change (CMCC) with a spatial resolution of 0.75° × 0.75° and a temporal resolution of 3 h. The SWAN model's boundary conditions were derived from the Model for Interdisciplinary Research on Climate (MRI-CGCM3) global wave projection model, which has a 1-degree spatial resolution and a 6-h temporal resolution and was developed by the Centre for Global Climate Research (CGCM). Therefore, a spatially varying boundary condition was defined, imposing incoming wave conditions for 28 locations with a 1-degree distance alongside the open boundary (Yukimoto et al., 2012). The boundary conditions were prepared assuming a JONSWAP (Joint North Sea Wave Project) spectrum (Mazzaretto et al., 2022), with the sea state conditions defined by the most relevant parameter for assessing the wave energy resource: significant wave height (H_{m0}), mean wave period, peak wave direction, and directional spreading. The choice of the JONSWAP spectrum was driven by its suitability for simulating wind-generated waves in the open ocean, which characterizes the conditions on the Atlantic coast of the Iberian Peninsula.

3. Results

The impact of climate change on the wave resource on the Atlantic coast of the Iberian Peninsula is investigated by comparing historical climate data (*His*) with climate projections for two timeframes (*Med* and *End*). The spatially varying analysis is conducted at the study domain scale and at the local scale, based on high-resolution wave model results. As mentioned earlier, three different 20-year timeframes (*His*, *Med*, and *End*) are considered in this study. The spatial plots in this section display the average wave power (P_w) for the considered timeframes, along with the differences between different timeframes. The spatial results suggest that the projected changes in wave parameters vary significantly among different seasons and over the year. In general, the winter and spring seasons show a greater decline in wave resources than the summer and

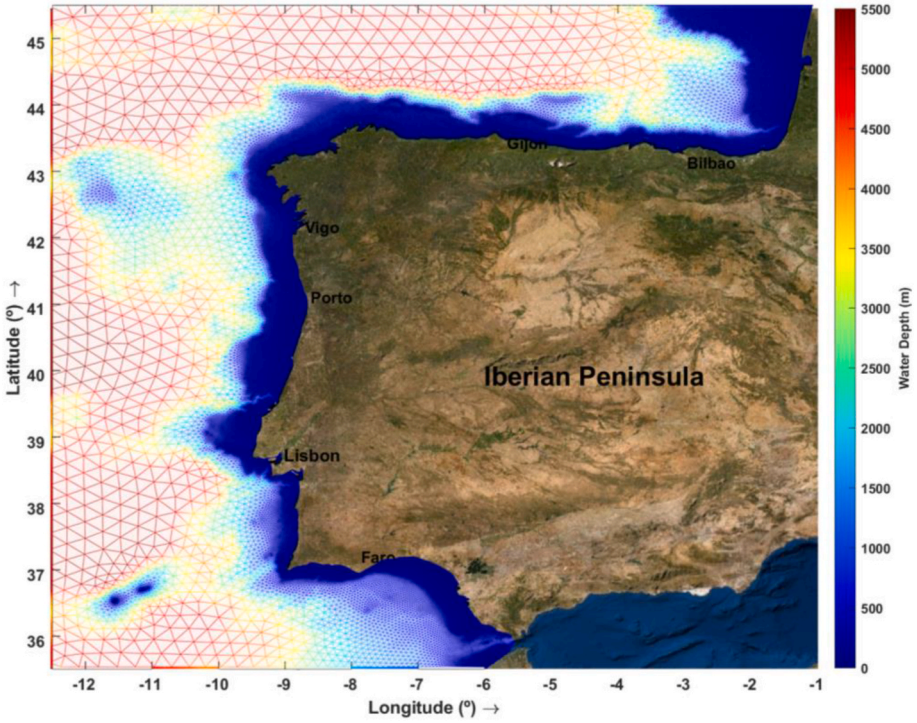

Fig. 1. The defined unstructured mesh grid system and bathymetry of the study area.

autumn seasons. The following section presents a detailed discussion of the results and their implications.

3.1. Spatial analysis

Fig. 2 shows the spatial distribution of the average P_w during the spring season and the deviation of the average P_w for *His*, *Med*, and *End* timeframes, with a focus on the Atlantic coastal region of the Iberian Peninsula.

According to the results shown in Fig. 2, the maximum P_w in the spring season in the region of study is 73.71 kW/m for the *His*, 62.15 kW/m for the *Med*, and 52.86 kW/m for the *End* timeframes, respectively. The highest P_w in all timeframes is presented at the northwest of the study area, while the lowest P_w is at the south and southwest. From the past to the future timeframes, as time goes forward, P_w decreases. The results shown in Fig. 2 also demonstrate a significant shift in the difference of P_w in the spring season. When comparing the *Med* and *His* timeframes, the maximum decrease was found to be 12.4 kW/m. Similarly, when comparing the *End* and *Med* timeframes, the maximum decrease was 9.29 kW/m, and when comparing the *End* to *His* data, the maximum decrease was 20.86 kW/m. These changes were found to be most prominent in the northwest region of the study domain, which has the highest P_w potential. Overall, the study domain shows a decrease during the spring season in all timeframes, except for a small area near the Strait of Gibraltar, where an increase of around 2 kW/m was observed in the difference between the *Med* and *His* timeframes.

Similarly, the spatial results of mean values of P_w and their corresponding deviations for the considered timeframes are presented in Fig. 3. The results shown in Fig. 3 present important findings on the variability of P_w in the summer season when considering different timeframes. The top row of Fig. 3 shows the variability of mean P_w in the study region for the *His*, *Med*, and *End* timeframes. The maximum P_w in the *His*, *Med*, and *End* timeframes were found to be 12.94 kW/m, 14.31 kW/m, and 14.28 kW/m, respectively. The highest P_w in the *His* time slice was found to be in the west of the study area, while the highest P_w for the *Med* and *End* were in the southwest of the study area. The lowest P_w was found to be in the southeast and northwest of the study area. When comparing the *Med* and *His* timeframes, the maximum increase was found to be 1.59 kW/m in the southwestern regions. Conversely, when comparing the *End* and *Med* timeframes, there is a maximum decrease of 1.83 kW/m in the northwest region, and when comparing the *End* and *His* timeframes, again, the maximum increase in the study area was found to be 2.57 kW/m in the southwest of the study domain. From the past to the future timeframes, the spatial distribution of P_w follows an opposite pattern in comparison with the spring season (Fig. 2), with the highest values of P_w concentrated in the southern regions of the study area and increasing slightly for the long-term horizon.

For the autumn season, the spatial distribution of the mean values of P_w, together with the difference for the different timeframes, are shown in Fig. 4.

The results obtained give significant insights into the variability of P_w in the autumn season when analyzed over different timeframes. The top row of Fig. 4 displays the fluctuations in the mean P_w in the study region for the *His*, *Med*, and *End* timeframes. The maximum mean P_w recorded in the *His*, *Med*, and *End* timeframes were 70.01 kW/m, 74.19 kW/m, and 60.06 kW/m, respectively. The highest P_w was observed in the northwest of the study area, while the lowest P_w was located in the southeast of the study area for all timeframes. Comparing the *Med* and *His* timeframes, it was found that there was an increase, in contrast to the summer and spring seasons (Figs. 2 and 3), with a maximum increase

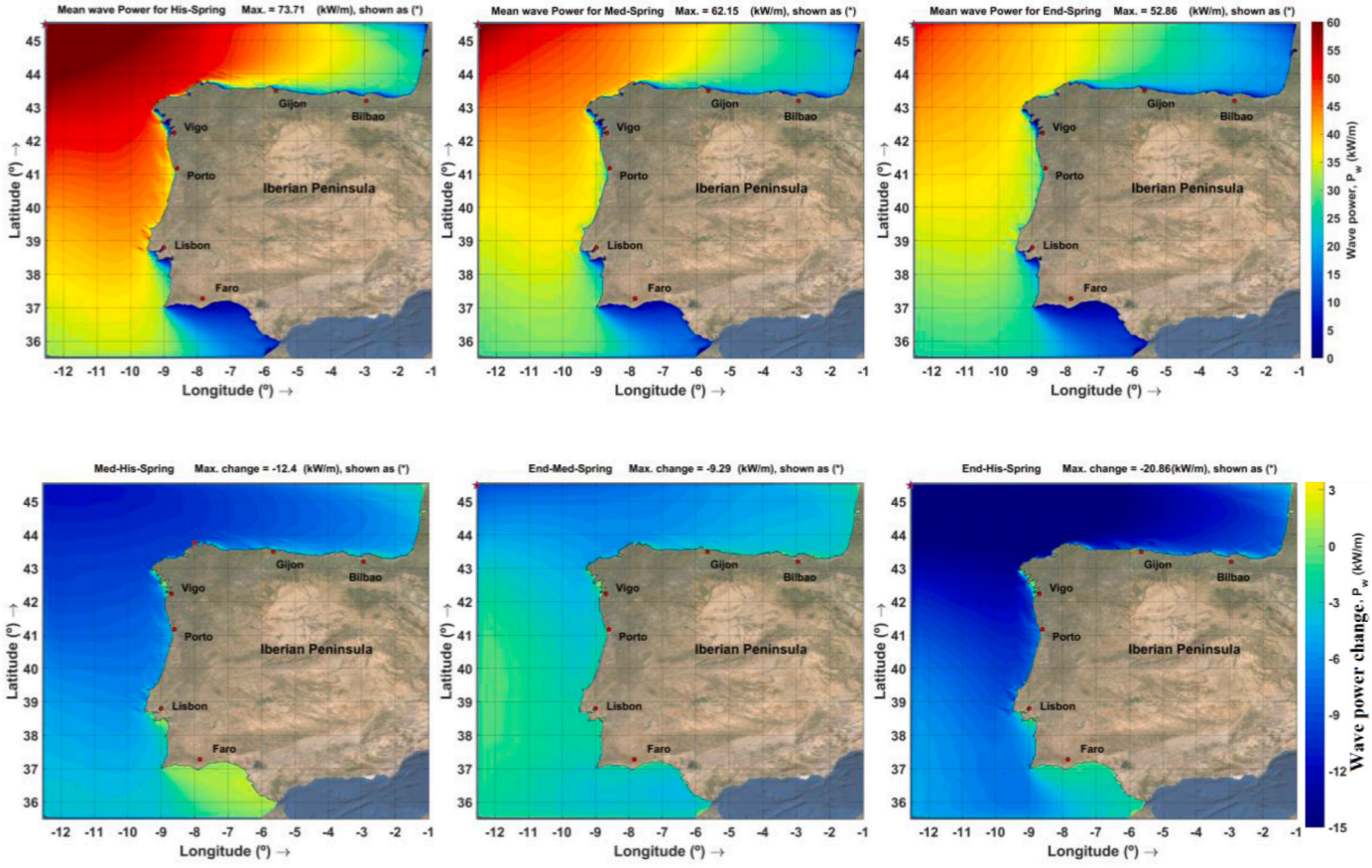

Fig. 2. The top row displays the spatial distribution of average P_w in kW/m for *His*, *Med*, and *End* (from left to right), while the bottom row exhibits the difference of average P_w in kW/m for *Med-His*, *End-Med*, and *End-His* timeframes (from left to right), during the spring season, respectively.

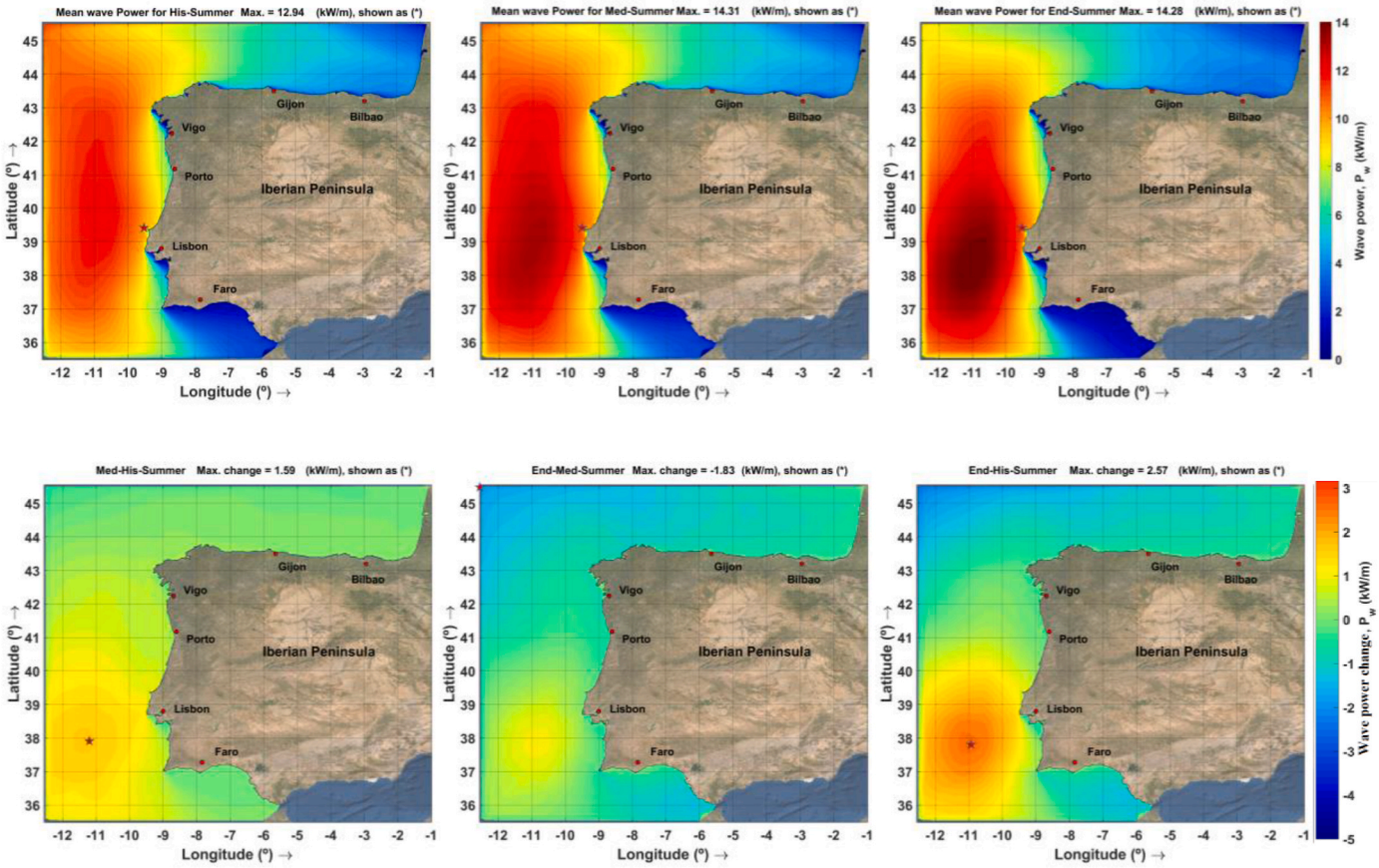

Fig. 3. The top row displays the spatial distribution of average P_w in kW/m for *His*, *Med*, and *End* (from left to right), while the bottom row exhibits the difference of average P_w in kW/m for *Med-His*, *End-Med*, and *End-His* timeframes (from left to right), during the summer season, respectively.

of 4.42 kW/m. However, when comparing the *End* and *Med* timeframes, a decrease was observed across the entire domain with a maximum decrease of 14.72 kW/m. Furthermore, when comparing the *End* and *His* datasets, a similar pattern emerged with a maximum decrease of 10.81 kW/m. During the autumn season, the most prominent increases or decreases were observed in the northwest region of the study domain, which presents the highest values of P_w during this timeframe.

Fig. 5 presents the results obtained for the winter regarding the spatial variation of mean values of P_w and the corresponding deviations between the different timeframes.

The top row of Fig. 5 shows the spatial changes of mean values of P_w for the *His*, *Med*, and *End* timeframes, which were found to be 158.00 kW/m, 131.69 kW/m, and 131.03 kW/m, respectively. The highest P_w in all timeframes was found in the northwest of the study area, while the lowest P_w was observed in the south and northeast of the study area. When comparing the *Med* and *His* datasets, the maximum decrease was found to be 26.31 kW/m, and when comparing the *End* and *His* timeframes, the maximum decrease was 26.97 kW/m. These changes were found to be most pronounced in the northwest region of the study domain, which has the highest P_w. The results demonstrate a general trend towards a decrease in P_w from the *His* to the *Med* and *End* timeframes. When comparing the *End* to the *Med*, the maximum decrease was 5.82 kW/m, with no significant changes observed across the rest of the study domain. It is worth noting that an increase in the difference of P_w was observed in the south of Portugal near the Strait of Gibraltar, where the *Med* and *His* data comparison indicates an increase of around 2 kW/m. The difference of *End-Med* in the winter season is also mostly presenting increased P_w across the entire study domain. The increased P_w in some seasons may have been caused by a regional increase in wind speed under the RCP8.5 climate change scenario.

Finally, the results for the annual analysis are presented in Fig. 6 and the results obtained reveal that the mean annual P_w distribution for the *His*, *Med*, and *End* timeframes reach the spatial maximum values of 78.27 kW/m, 69.71 kW/m, and 63.23 kW/m, respectively. The higher values of P_w across all timeframes were observed in the northwest region of the study area, while the lower values of P_w were found in the south and northeast of the study area. When comparing the *Med* to the *His* data, the maximum decrease in P_w observed is 8.56 kW/m. Similarly, the comparison between the *End* and *Med* datasets showed a maximum decrease of 7.18 kW/m. Lastly, the comparison of the *End* and *His* timeframes revealed a maximum decrease in P_w of 15.05 kW/m. These decreases in P_w were found to be most prominent in the northwest region of the study domain, which has the highest P_w potential. The results of the study indicate a general trend towards a decrease in P_w from the *His* to the *Med* and *End* timeframes. Overall, the study results demonstrate a decrease in P_w over the annual time scale in all timeframes. The decline in P_w can be attributed to the climate projections under the RCP8.5 emission scenario and the corresponding increased warming.

3.2. Local analysis

In order to gain a more thorough understanding of the time-series of mean P_w and wave directions, a representative nearshore location, longitude of −8.829°W, and latitude of 41.511°N, at 32 m water depth, was chosen to conduct a local analysis. The intra-annual mean P_w at this location is shown in Fig. 7.

Through analysis of the moving average P_w shown in Fig. 7, it can be observed that: *His* has the highest average wave power throughout the year, except in late February where it is the lowest. This suggests that the wave power decreased slightly in late February compared to the rest of

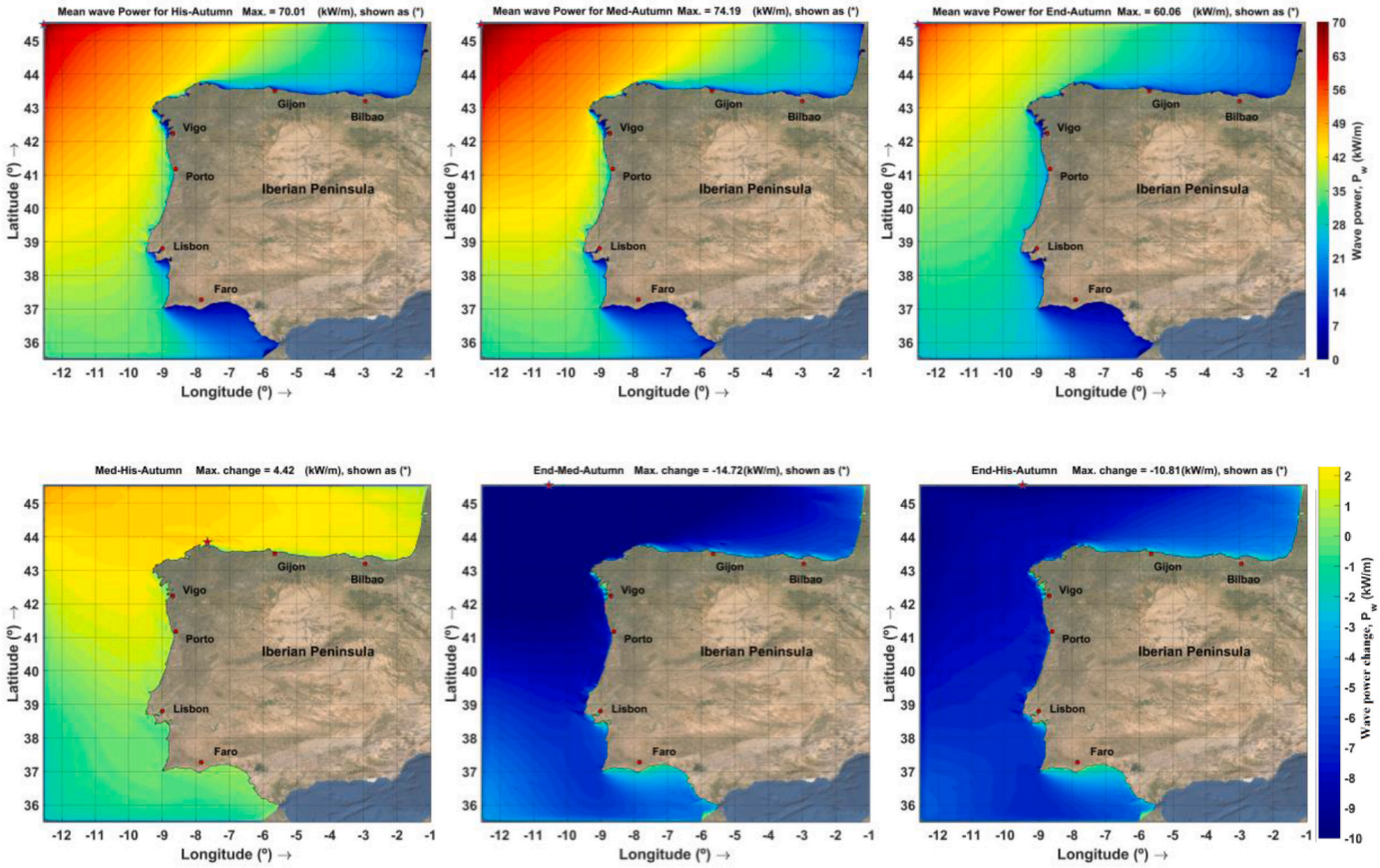

Fig. 4. The top row displays the spatial distribution of average P_w in kW/m for *His*, *Med*, and *End* (from left to right), while the bottom row exhibits the difference of average P_w in kW/m for *Med-His*, *End-Med*, and *End-His* timeframes (from left to right), during the autumn season, respectively.

the year. *Med* has the lowest average P_w in the first half of January, but then it increases rapidly to become the highest in late February to early March. This peak in P_w coincides with a dip in P_w for *His*. After March, *Med* gradually decreases in P_w until it becomes the lowest again in April. It then remains in the middle of the two time-series until November, when it becomes the highest until the end of the year. This suggests that there is a seasonal variation in wave power for *Med*. *End* is in the middle of the two time-series for most of the year, except for the first half of February where it is the lowest, and the first 10 days of December where it is the highest. This suggests that there are brief periods of higher and lower wave power for *End*.

Based on these observations, it appears that there are distinct patterns in the P_w time-series for each of the three timeframes. The *His* time-series consistently shows the highest P_w values throughout the year, while the *Med* and *End* time-series show more variation, with *Med* being highest during late winter and early spring. These differences suggest that P_w may be affected by a range of factors, including seasonal changes, regional variations, and the RCP8.5 climate change pattern.

Fig. 8 presents the exceedance percentiles of H_{m0} and energy period (T_e) for the same nearshore location, in order to provide an understanding of the distribution of the accumulated data (58440 values) over 20 years for the *His*, *Med*, and *End* timeframes.

The 50th exceedance probability values of H_{m0} exhibit a downward trend from 1.94 m to 1.90 m and to 1.82 m, for the *His*, *Med,* and *End* timeframes, respectively. Similarly, the 5th exceedance probability values of H_{m0} decrease from 4.49 m to 4.24 m and 4.06 m, for the timeframes of *His*, *Med,* and *End*, respectively. These findings suggest a decrease in the average values of H_{m0} over time, as demonstrated by the reduction in both the 50th and 5th exceedance percentiles from the *His* to *End* timeframes.

Likewise, the 50th exceedance probability values of T_e exhibit a decreasing trend from 9.22 s to 9.18 s and 9.04 s, for the *His*, *Med,* and *End* timeframes, respectively. The 5th exceedance probability values of T_e also show a decreasing trend (ranging from 14.15 s to 13.87 s and 13.70 s for the *His*, *Med,* and End timeframes, respectively). Consequently, the results obtained suggest a decline in the average values of H_{m0} and T_e over time, as evidenced by the decrease in both the 50th and 5th exceedance percentiles from *His* to *End*. The wave roses in Fig. 9 illustrate the directional characteristics of waves with different H_{m0} during *His*, *Med*, and *End* timeframes at the study location.

The wave roses in Fig. 9 reveal that the dominant wave direction remains constant across all three timeframes, with the highest occurrence of waves coming from the west. However, as time advances from *His* to *End*, a reduction in wave heights can be observed, as indicated by the colormap of the wave rose plot. Furthermore, in the outer circle of the wave roses, the percentage of waves with a west direction exhibits a decline from 65% for the *His* timeframe to 57% for the *Med* timeframe and further to 55% for the *End* timeframe. This suggests a shift in the incoming wave direction over time (with a larger number of waves presenting an incoming Northwest direction). Moreover, the percentages of waves with magnitudes below 3 m coming from the northwest for the *His*, *Med*, and *End* timeframes are 33%, 38%, and 42%, respectively. This indicates a relative increase in the frequency of occurrence of these waves as time progresses from *His* to *End*. Overall, these findings demonstrate a shift in the wave climate over time, with a decrease in wave heights and a change in the relative proportions of wave directions.

The findings of this study reveal a dominant wave direction from the west across all three timeframes, consisting of a total of 58,440 data points. However, the expected dominant wave direction in this location,

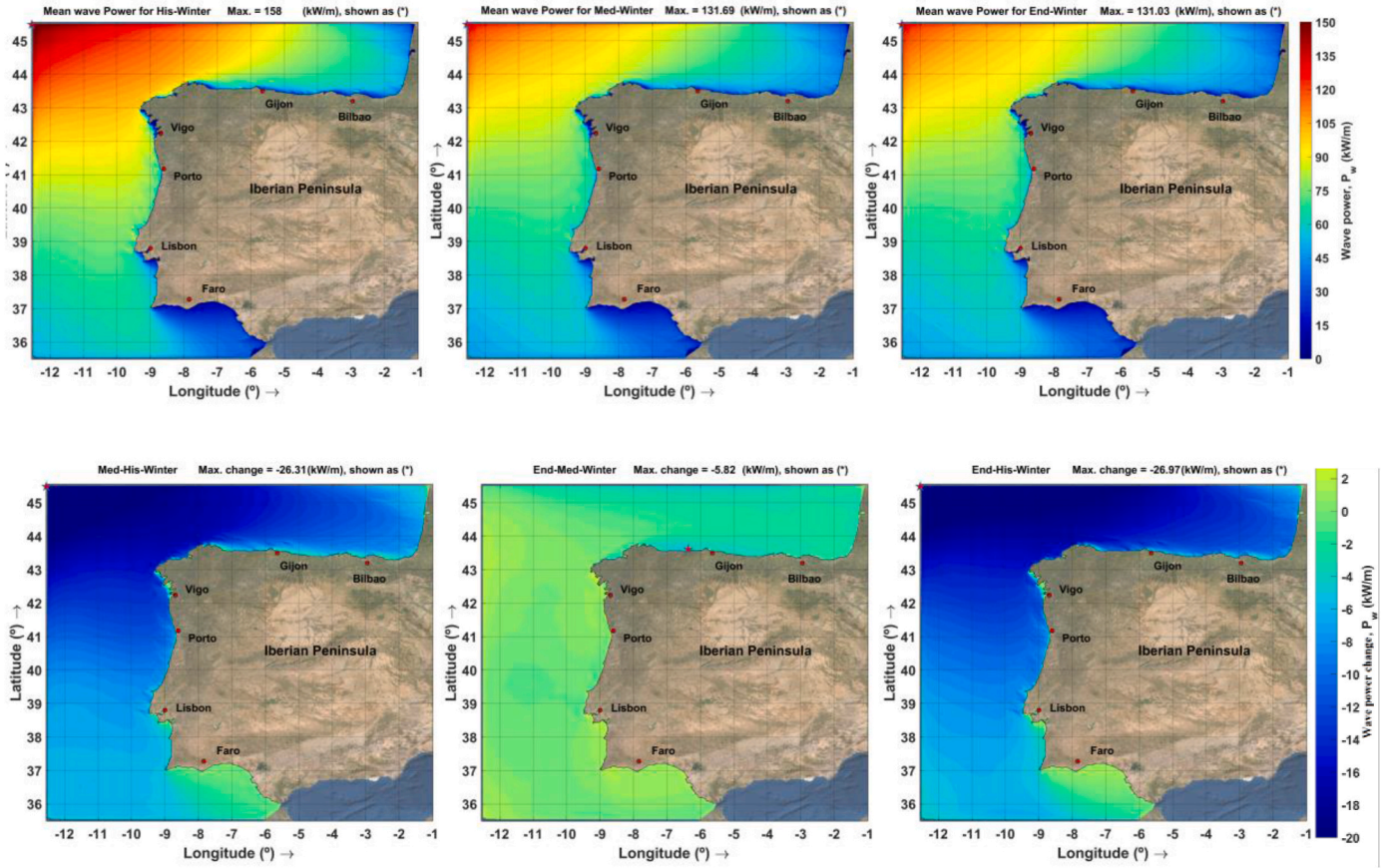

Fig. 5. The top row displays the spatial distribution of average P_w in kW/m for *His*, *Med*, and *End* (from left to right), while the bottom row exhibits the difference of average P_w in kW/m for *Med-His*, *End-Med*, and *End-His* timeframes (from left to right) during the winter season, respectively.

based on reanalysis data, is from the northwest. This discrepancy may be attributed to potential inaccuracies in the climate projection scenario RCP8.5 used in this study. It is important to acknowledge that uncertainties and limitations in climate projection scenarios can impact the accuracy of wave direction predictions. Furthermore, other factors such as local variations, geographical features, temporal fluctuations, and unanticipated changes in the climate system may also contribute to the observed deviation. Additionally, it is noteworthy that the objective of this study is to conduct a comparative analysis of outcomes generated by a singular climate projection model and evaluate the variations that may arise across various time periods.

Table 1 (*Med-His*), 2 (*End-Med*), and 3 (*End-His*) provide a comparison of the wave resource matrices for the chosen location between the timeframes considered in this study. The objective of these tables is to provide insight into the changes projected to occur in the different sea states over time.

The presented difference matrices of the wave resources in Tables 1–3 suggest that the wave power levels on the Atlantic coast of the Iberian Peninsula will change in the future under the RCP8.5 climate change scenario. Each cell of the tables corresponds to specific ranges of H_{m0} and T_e and the positive values (%) are roughly ranged between H_{m0} (2–5 m) and T_e (6–10 s), H_{m0} (1–2 m) and T_e (4–6 s), and H_{m0} (2–4 m) and T_e (4–13 s) for Tables 1–3, respectively. Positive values in each table indicate an increase in the probability of occurrence for the corresponding sea states, while negative values indicate a decrease in the probability of occurrence for the corresponding sea state. There is a decreasing trend for higher H_{m0} and T_e values, particularly for cells with less probability of occurrence, suggesting that the extreme sea states are decreasing in the future. On the other hand, an increasing trend is observed in sea states for waves with lower H_{m0} and T_e values.

It is important to note that the difference may vary across locations and timeframes, and can be influenced by local bathymetry, wind patterns, and other site-specific characteristics. Therefore, these analyses should be considered when applying WECs to understand the impact of climate change on the specific sea state classes dominant in the power matrix of the selected WEC at the location of interest.

4. Discussion

A high-resolution unstructured wave model was successfully applied, after calibration and validation against field data from 10 different locations across the study area (Majidi et al., 2023). This approach allowed a very detailed examination of climate change's impact on wave energy resources at both regional and local scales. A comprehensive overview of projected changes on annual and intra-annual scales was achieved by comparing three different timeframes.

Due to uncertainties associated with climate change projections, in this work, it was decided to study the most extreme climate change scenario to obtain conservative outcomes (i.e., "upper boundary" of expected changes). Uncertainties are present in all works dealing with projections; therefore this "limitation" applies to projections based on RCP8.5 and the other scenarios.

A notable decrease in wave power over the various timeframes was observed in this study, with the reduction being more pronounced during winter and spring seasons compared to summer and autumn. Higher P_w values were consistently registered in the northwest region. An unexpected increment in P_w in the vicinity of the Strait of Gibraltar was noted when the Med to His timeframes were compared, potentially attributed to regional increases in wind speed under the RCP8.5 climate change scenario.

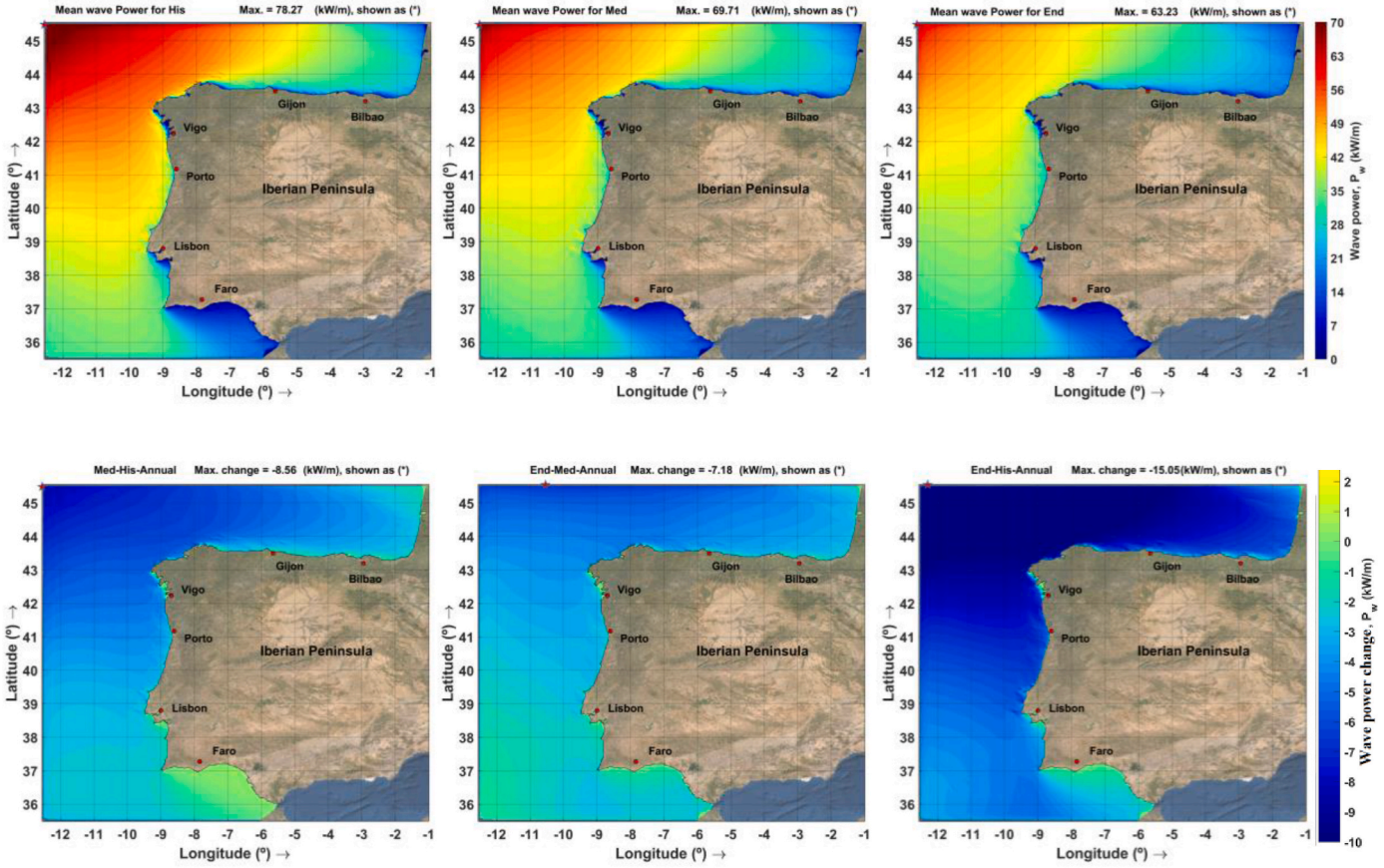

Fig. 6. The top row displays the spatial distribution of average P_w in kW/m for *His*, *Med*, and *End* (from left to right), while the bottom row exhibits the difference of average P_w in kW/m for *Med-His*, *End-Med*, and *End-His* timeframes (from left to right), during the whole year, respectively.

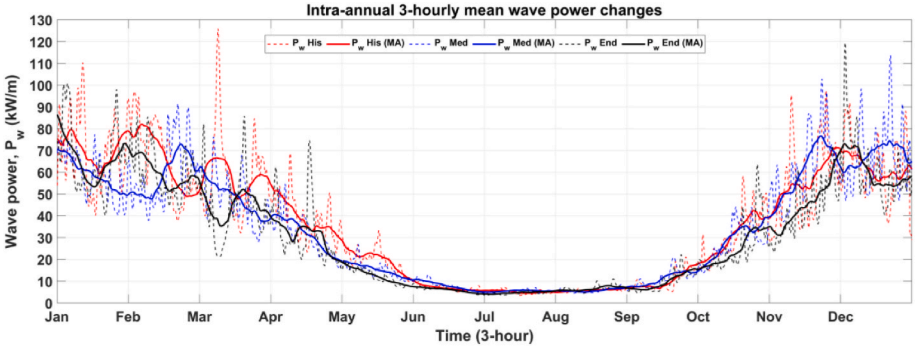

Fig. 7. The 3-hourly time-series and moving average with a window size of 100 point-data for mean P_w for *His*, *Med,* and *End*.

Previous works, such as that of Rusu (2022) projected near-future (2026–2045) wave power using the less severe RCP4.5 scenario, while Ribeiro et al. (2020) investigated the near-future hybrid wind-wave energy resource for the northwest coast of Iberian Peninsula using a Delphi method to classify wind and wave energy resources between 2026 and 2045. The relevance of these findings for the wave energy community is clear, highlighting potential future challenges for the wave energy industry in the long term under the severe RCP8.5 climate change scenario.

Compared to previous research work, a distinctive feature of the present study is that it provides a comprehensive examination of the impact of the RCP8.5 climate change scenario on the wave resources along the Atlantic coast of the Iberian Peninsula, employing a high-resolution and unstructured meshed SWAN model. Spatial variations of this impact under the severe RCP8.5 scenario were explored, highlighting that climate change effects can vary significantly between regions.

Under the RCP8.5 scenario, it was inferred that climate change could lead to a decrease in the wave power resource along the Atlantic coast of the Iberian Peninsula. This reduction could be associated with predicted lower regional changes in atmospheric pressure due to global warming, which could decrease wind speeds and consequently the energy driving ocean waves. This decrease in wind speeds, in turn, results in a decline in the energy that boosts ocean waves, ultimately leading to lower values of P_w (Pryor et al., 2020; National Geography, 2023). It is important to note that the decrease in P_w has implications for wave energy farms. Therefore, it is crucial to monitor and assess the changes in P_w as a result of climate change in order to adapt and plan accordingly for future

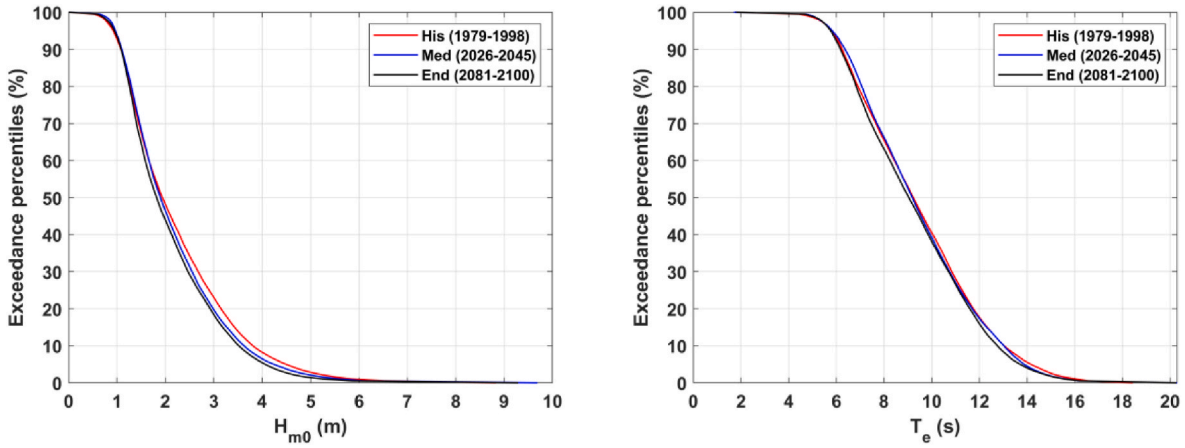

Fig. 8. The exceedance percentiles of H_{m0} (left plot) and T_e (right plot) for *His*, *Med,* and *End* data series.

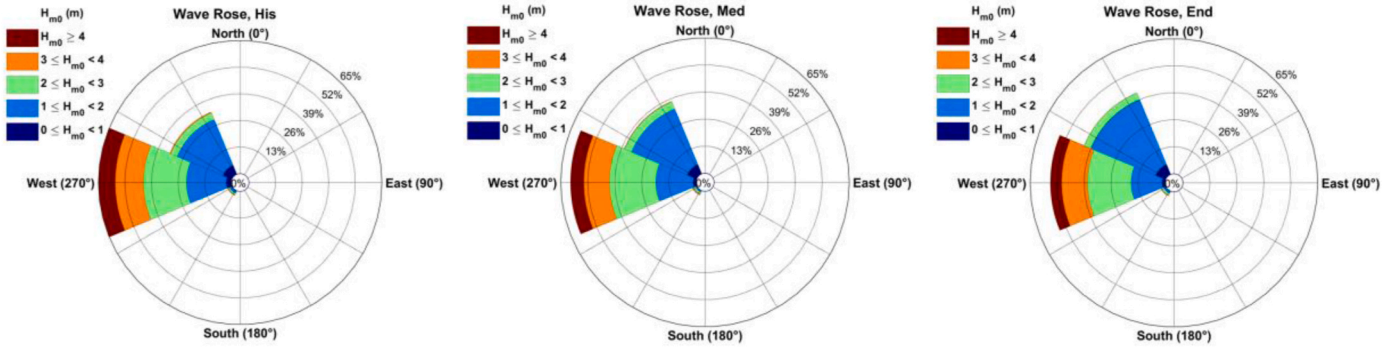

Fig. 9. The wave rose of incoming waves at the chosen location for *His* (left plot), *Med* (middle plot), and *End* (right plot).

Table 1
The difference of the wave resource matrix (%) of *Med* compared to *His* at the selected location (*Med–His*).

		T_e (s)																
		0	**1**	**2**	**3**	**4**	**5**	**6**	**7**	**8**	**9**	**10**	**11**	**12**	**13**	**14**	**15**	**16**	**17**
H_{m0} **(m)**	**0**		0.01	-0.01	-0.05	-0.09	-0.07	-0.03											
	1			-0.01	-0.18	-0.02	-0.22	-0.35	-0.05	-0.05	0.03	0.01							
	2				0.02	-0.16	-0.44	0.40	0.51	-0.14	-0.03	-0.05	0.01	0.01					
	3						-0.21	-0.06	0.54	0.98	0.79	0.32	0.17	0.09	0.04	0.01			
	4						-0.02	-0.06	0.22	0.23	0.17	0.22	0.04	0.19	0.20	0.02			
	5							0.01	0.12	0.11	-0.19	-0.37	0.03	0.47	0.26	-0.01	-0.01		
	6								0.01	-0.02	-0.15	-0.34	-0.39	-0.04	0.05	-0.08	-0.01	-0.02	
	7								-0.01	-0.08	-0.12	-0.15	-0.19	-0.07	0.03		-0.02	-0.01	
	8									-0.03	-0.12	-0.05	-0.10	-0.17		0.03	-0.04	-0.05	-0.01
	9									-0.01	-0.04	-0.03	-0.01	-0.07	-0.09	-0.07	-0.08	-0.04	
	10											-0.03	-0.03	-0.01	-0.04	-0.08	-0.08	-0.04	
	11										0.01		-0.01	-0.02	-0.03	-0.03	-0.02	-0.02	-0.01
	12														-0.05	-0.04	-0.01	-0.01	
	13												-0.01	-0.01	-0.01	-0.03	-0.02	-0.01	
	14															-0.02	-0.02	-0.01	
	15																-0.01	-0.01	

developments of WECs and wave farms.

In summary, significant implications arise for the wave energy sector, especially for farms to be situated along the Atlantic coast of the Iberian Peninsula. The projected decrease in wave power calls for strategic positioning of wave energy converters to optimize performance under changing conditions. In this context, future research is suggested to incorporate more diverse climate projection scenarios, capturing a wider range of potential outcomes.

5. Conclusion

In general, the present study provides valuable insights into the potential impacts of climate change on the wave resource (P_w) on the Atlantic coast of the Iberian Peninsula. The findings attained indicate a potential decline in the wave energy resource, more pronounced in the northwestern region, emphasizing the urgency of further research and strategic planning in wave energy sectors, particularly in regions of significant wave power reductions.

The results indicate an overall decrease in P_w over time, except for

Table 2
The difference of the wave resource matrix (%) of *End* compared to *Med* at the selected location (*End* – *Med*).

		T_e (s)																
		0	**1**	**2**	**3**	**4**	**5**	**6**	**7**	**8**	**9**	**10**	**11**	**12**	**13**	**14**	**15**	**16**	**17**
H_{m0} **(m)**	**0**				0.01	0.03	0.03		-0.01										
	1			-0.01	0.05	-0.10	0.24	0.36	-0.07	-0.08	-0.05								
	2					0.79	1.52	0.57	0.04	0.34	0.07	-0.05	0.03	0.02					
	3					-0.01	0.10	0.02	-0.42	-0.56	-0.32	-0.09	0.01	0.04	0.03	0.02	0.01	0.01	
	4						-0.01	-0.04	-0.28	-0.38	-0.22	0.17	0.32		-0.06	0.03	0.02		
	5							-0.04	-0.12	-0.07	-0.08	-0.11	-0.03	-0.21	-0.17	0.01	-0.02	-0.01	
	6							-0.01	-0.03	-0.16	-0.05	0.19	0.29	0.04	-0.16	-0.03	-0.01	0.01	
	7								-0.01	-0.06	-0.02	0.13	0.04	-0.20	-0.21	-0.02	0.07		
	8									-0.03	-0.04	0.01	0.10	0.09	-0.04	-0.07	-0.01		-0.01
	9										-0.03	-0.07	-0.06	-0.09	-0.08	-0.03	-0.01	0.01	
	10										-0.02	-0.02	-0.02	-0.08	-0.12	-0.06		0.01	
	11										-0.01	-0.01	-0.02	-0.04	-0.05	-0.06	-0.03		
	12												-0.01	-0.03	-0.01	-0.02	-0.01	0.02	
	13															-0.02	-0.03	-0.01	
	14																-0.01	-0.01	-0.01
	15																		

Table 3
The difference of the wave resource matrix (%) of *End* compared to *His* at the selected location (*End* – *His*).

		T_e (s)																
		0	**1**	**2**	**3**	**4**	**5**	**6**	**7**	**8**	**9**	**10**	**11**	**12**	**13**	**14**	**15**	**16**	**17**
H_{m0} **(m)**	**0**			-0.01	-0.04	-0.06	-0.05	-0.03	-0.01										
	1			-0.02	-0.12	-0.12	0.01	0.01	-0.12	-0.13	-0.02								
	2				0.02	0.63	1.08	0.97	0.55	0.21	0.04	-0.11	0.04	0.03					
	3					-0.02	-0.10	-0.04	0.12	0.41	0.47	0.23	0.19	0.13	0.06	0.03	0.01	0.01	
	4						-0.03	-0.10	-0.06	-0.15	-0.05	0.39	0.37	0.19	0.14	0.05	0.02		
	5							-0.03		0.04	-0.27	-0.47	-0.01	0.26	0.10		-0.03	-0.01	
	6								-0.02	-0.18	-0.21	-0.15	-0.10		-0.11	-0.11	-0.02	-0.01	
	7								-0.02	-0.14	-0.14	-0.02	-0.15	-0.26	-0.19	-0.02	0.04	-0.01	
	8									-0.06	-0.17	-0.04		-0.07	-0.04	-0.05	-0.06	-0.05	-0.01
	9									-0.01	-0.07	-0.09	-0.07	-0.16	-0.17	-0.11	-0.09	-0.03	-0.01
	10										-0.02	-0.05	-0.05	-0.09	-0.15	-0.14	-0.08	-0.03	
	11											-0.01	-0.03	-0.05	-0.08	-0.08	-0.05	-0.03	-0.01
	12												-0.01	-0.03	-0.05	-0.06	-0.02	0.01	
	13												-0.01	-0.01	-0.02	-0.05	-0.05	-0.02	-0.01
	14															-0.02	-0.03	-0.02	-0.01
	15															-0.01	-0.02	-0.02	-0.01

the area situated in the southern region of Portugal near the Strait of Gibraltar, where an increase in P_w is expected in future timeframes. This trend is attributed to the projected increase in global warming and the associated decrease in the local wind speeds, which may be caused by a reduction in changes in regional atmospheric pressure. The decrease in P_w over time may result in decreases in energy production and reduced economic benefits for wave energy investors. Changes in P_w may also have an impact on coastal infrastructure, as lower wave energy may result in reduced wave-loading on coastal structures. Therefore, the findings of this study emphasize the need to further consider the implications of changing P_w on both wave energy production and coastal infrastructure.

The numerical wave model used in this study, along with the high-resolution and long-term assessment of wave resources, provides an important contribution to the understanding of P_w in the Atlantic coastal region of the Iberian Peninsula. By utilizing the SWAN model with the high-resolution unstructured mesh, the study could capture the complex dynamics of wave propagation in the region.

Overall, this study provides a useful foundation for future research on P_w in the Atlantic coastal area of the Iberian Peninsula, particularly in the face of a changing climate. It highlights the importance of continued research and monitoring to plan and understand the impact of climate change on the P_w generation. Coastal communities and wave energy power plants must be prepared to adapt to potential changes in P_w. Finally, the findings in this study have important implications for the sustainable development of the coastal regions in the Iberian Peninsula.

Declaration of competing interest

The authors declare that they have no known competing financial interests or personal relationships that could have appeared to influence the work reported in this paper.

Data availability

The data that has been used is confidential.

Acknowledgments

The authors acknowledge funding in the form of a Ph.D. scholarship grant by the Portuguese Foundation of Science and Technology (FCT), co-financed by the EU's ESF through the NORTE 2020 program, with reference 2021.04847.BD. This work was also supported by the project WEC4Ports – A hybrid Wave Energy Converter for Ports (OCEANERA-NET COFUND, with the reference OCEANERA/0004/2019) funded under the frame of FCT, and the project ATLANTIDA (NORTE-01-0145-FEDER-000040), supported by the North Portugal Regional Operational Programme (NORTE2020), under the PORTUGAL 2020 Partnership Agreement and through the European Regional Development Fund (ERDF). Furthermore, during this research study, Victor Ramos was supported by the program of Stimulus of Scientific Employment Individual Support (CEECIND/03665/2018) from FCT and Gianmaria Giannini was supported by the individual grant No: 2022.04954.

CEECIND by FCT. Also, the authors greatly appreciate the valuable support of Prof. Adem Akpinar and Dr. Khalid Amarouche during the study.

References

Amarouche, K., Akpınar, A., Soran, M.B., Myslenkov, S., Majidi, A.G., Kankal, M., Arkhipkin, V., 2021. Spatial calibration of an unstructured SWAN model forced with CFSR and ERA5 winds for the Black and Azov Seas. Appl. Ocean Res. 117, 102962 https://doi.org/10.1016/J.APOR.2021.102962.

AW-Energy. Waveroller. URL. https://aw-energy.com/waveroller/. (Accessed 7 June 2023).

Bingölbali, B., Majidi, A.G., Akpınar, A., 2021. Inter- and intra-annual wave energy resource assessment in the south-western Black Sea coast. Renew. Energy 169, 809–819. https://doi.org/10.1016/J.RENENE.2021.01.057.

Booij, N., Ris, R.C., Holthuijsen, L.H., 1999. A third-generation wave model for coastal regions: 1. Model description and validation. J Geophys Res Oceans 104, 7649–7666. https://doi.org/10.1029/98JC02622.

Charles, E., Idier, D., Delecluse, P., Déqué, M., Le Cozannet, G., 2012. Climate change impact on waves in the bay of Biscay, France. Ocean Dynam. 62, 831–848. https://doi.org/10.1007/S10236-012-0534-8/FIGURES/11.

Chini, N., Stansby, P., Leake, J., Wolf, J., Roberts-Jones, J., Lowe, J., 2010. The impact of sea level rise and climate change on inshore wave climate: a case study for East Anglia (UK). Coast. Eng. 57, 973–984. https://doi.org/10.1016/J.COASTALENG.2010.05.009.

CorPower Ocean. Wave Energy. To Power the Planet. URL. https://corpowerocean.com/wave-energy/. (Accessed 7 June 2023).

Dietrich, J.C., Tanaka, S., Westerink, J.J., Dawson, C.N., Luettich, R.A., Zijlema, M., Holthuijsen, L.H., Smith, J.M., Westerink, L.G., Westerink, H.J., 2012. Performance of the unstructured-mesh, SWAN+ ADCIRC model in computing hurricane waves and surge. J. Sci. Comput. 52, 468–497. https://doi.org/10.1007/S10915-011-9555-6/METRICS.

Eco Wave Power - Wave Energy Company, URL https://www.ecowavepower.com/(accessed 7.June.2023).

Goharnejad, H., Nikaein, E., Perrie, W., 2021. Assessment of wave energy in the Persian Gulf: an evaluation of the impacts of climate change. Oceanologia 63, 27–39. https://doi.org/10.1016/J.OCEANO.2020.09.004.

Harsher, R., 2023. Climate Change Causes More Severe Weather. URL. https://www.npr.org/2023/01/09/1147805696/climate-change-makes-heat-wavesstorms-and-droughts-worse-climate-report-confirm. (Accessed 30 April 2023).

Lavaa, 2023. Wave energy advantages and disadvantages. Update), URL. https://www.linquip.com/blog/wave-energy-advantages-disadvantages/. (Accessed 4 December 2023).

Hersbach, H., Bell, B., Berrisford, P., Hirahara, S., Horányi, A., Muñoz-Sabater, J., Nicolas, J., Peubey, C., Radu, R., Schepers, D., Simmons, A., Soci, C., Abdalla, S., Abellan, X., Balsamo, G., Bechtold, P., Biavati, G., Bidlot, J., Bonavita, M., De Chiara, G., Dahlgren, P., Dee, D., Diamantakis, M., Dragani, R., Flemming, J., Forbes, R., Fuentes, M., Geer, A., Haimberger, L., Healy, S., Hogan, R.J., Hólm, E., Janisková, M., Keeley, S., Laloyaux, P., Lopez, P., Lupu, C., Radnoti, G., de Rosnay, P., Rozum, I., Vamborg, F., Villaume, S., Thépaut, J.N., 2020. The ERA5 global reanalysis. Q. J. R. Meteorol. Soc. 146, 1999–2049. https://doi.org/10.1002/QJ.3803.

Hoque, M.A., Perrie, W., Solomon, S.M., 2020. Application of SWAN model for storm generated wave simulation in the Canadian Beaufort Sea. J. Ocean Eng. Sci. 5, 19–34. https://doi.org/10.1016/j.joes.2019.07.003.

Li, N., Cheung, K.F., Stopa, J.E., Hsiao, F., Chen, Y.L., Vega, L., Cross, P., 2016. Thirty-four years of Hawaii wave hindcast from downscaling of climate forecast system reanalysis. Ocean Model. 100, 78–95. https://doi.org/10.1016/J.OCEMOD.2016.02.001.

Lionello, P., Cogo, S., Galati, M.B., Sanna, A., 2008. The Mediterranean surface wave climate inferred from future scenario simulations. Global Planet. Change 63, 152–162. https://doi.org/10.1016/J.GLOPLACHA.2008.03.004.

Luettich, R.A., Richard, A., Westerink, J.J., Scheffner, N.W., 1992. ADCIRC : an advanced three-dimensional circulation model for shelves, coasts, and estuaries. Report 1, Theory and methodology of ADCIRC-2DD1 and ADCIRC-3DL (Tech. Rep. No DRP-92-6), pp. 1–137.

Majidi, A.G., Bingölbali, B., Akpınar, A., 2020. Power production performance of different wave energy converters in the southwestern Black Sea. Int. J. Energy Power Eng. 14, 191–195.

Majidi, A.G., Bingölbali, B., Akpınar, A., Iglesias, G., Jafali, H., 2021a. Downscaling wave energy converters for optimum performance in low-energy seas. Renew. Energy 168, 705–722. https://doi.org/10.1016/J.RENENE.2020.12.092.

Majidi, A.G., Bingölbali, B., Akpınar, A., Rusu, E., 2021b. Wave power performance of wave energy converters at high-energy areas of a semi-enclosed sea. Energy 220, 119705. https://doi.org/10.1016/J.ENERGY.2020.119705.

Majidi, A.G., Ramos, V., Amarouche, K., Rosa Santos, P., das Neves, L., Taveira-Pinto, F., 2023. Assessing the impact of wave model calibration in the uncertainty of wave energy estimation. Renew. Energy. https://doi.org/10.1016/J.RENENE.2023.05.049.

Majidi, A.G., Bingölbali, B., Akplnar, A., 2020a. The changes of theoretical wave power from offshore to coast in the south-western Black Sea. In: E3S Web of Conferences, 191, 03004. https://doi.org/10.1051/E3SCONF/202019103004.

Majidi, A.G., Bingölbali, B., Akplnar, A., Rusu, E., 2020b. Dimensionless normalized wave power in the hot-spot areas of the Black Sea. In: E3S Web of Conferences, 173, 01001. https://doi.org/10.1051/E3SCONF/202017301001.

Mazzaretto, O.M., Menéndez, M., Lobeto, H., 2022. A global evaluation of the JONSWAP spectra suitability on coastal areas. Ocean Eng. 266, 112756 https://doi.org/10.1016/J.OCEANENG.2022.112756.

Mazzolari, A., 2013. Two Dimensional Unstructured Mesh Generation Applied to Shallow Water Models (Doctoral Dissertation. PhD Thesis. Department of Civil Engineering. Instituto Superior Técnico, Lisbon).

Mørk, G., Barstow, S., Kabuth, A., Pontes, M.T., 2010. Assessing the global wave energy potential. In: Proceedings of the International Conference on Offshore Mechanics and Arctic Engineering, 3. OMAE, pp. 447–454. https://doi.org/10.1115/OMAE2010-20473.

National Geography. Wind. URL. https://education.nationalgeographic.org/resource/wind/. (Accessed 7 June 2023).

Pavlova, A., Myslenkov, S., Arkhipkin, V., Surkova, G., 2022. Storm surges and extreme wind waves in the caspian sea in the present and future climate. Civil Engineering Journal 8, 2353–2377. https://doi.org/10.28991/CEJ-2022-08-11-01.

Pourali, M., Kavianpour, M.R., Kamranzad, B., Alizadeh, M.J., 2023. Future variability of wave energy in the Gulf of Oman using a high resolution CMIP6 climate model. Energy 262, 125552. https://doi.org/10.1016/J.ENERGY.2022.125552.

Pryor, S.C., Barthelmie, R.J., Bukovsky, M.S., Leung, L.R., Sakaguchi, K., 2020. Climate change impacts on wind power generation. Nat. Rev. Earth Environ. 1 (12 1), 627–643. https://doi.org/10.1038/s43017-020-0101-7, 2020.

Ramos, V., López, M., Taveira-Pinto, F., Rosa-Santos, P., 2017. Influence of the wave climate seasonality on the performance of a wave energy converter: a case study. Energy 135, 303–316. https://doi.org/10.1016/J.ENERGY.2017.06.080.

Reeve, D.E., Chen, Y., Pan, S., Magar, V., Simmonds, D.J., Zacharioudaki, A., 2011. An investigation of the impacts of climate change on wave energy generation: the Wave Hub, Cornwall, UK. Renew. Energy 36, 2404–2413. https://doi.org/10.1016/J.RENENE.2011.02.020.

Reguero, B.G., Losada, I.J., Méndez, F.J., 2019. A recent increase in global wave power as a consequence of oceanic warming. Nat. Commun. 10 (1 10), 1–14. https://doi.org/10.1038/s41467-018-08066-0, 2019.

Riahi, K., Rao, S., Krey, V., Cho, C., Chirkov, V., Fischer, G., Kindermann, G., Nakicenovic, N., Rafaj, P., 2011a. RCP 8.5-A scenario of comparatively high greenhouse gas emissions. Clim. Change 109, 33–57. https://doi.org/10.1007/S10584-011-0149-Y.

Riahi, K., Rao, S., Krey, V., Cho, C., Chirkov, V., Fischer, G., Kindermann, G., Nakicenovic, N., Rafaj, P., 2011b. RCP 8.5-A scenario of comparatively high greenhouse gas emissions. Clim. Change 109, 33–57. https://doi.org/10.1007/S10584-011-0149-Y/FIGURES/12.

Ribeiro, A., Costoya, X., de Castro, M., Carvalho, D., Dias, J.M., Rocha, A., Gomez-Gesteira, M., 2020. Assessment of hybrid wind-wave energy resource for the NW coast of iberian Peninsula in a climate change context. Applied Sciences 2020 10 (10), 7395. https://doi.org/10.3390/APP10217395, 7395.

Rodríguez-Martín, J., Cruz-Pérez, N., Santamarta, J.C., 2022. Maritime climate in the canary Islands and its implications for the construction of coastal infrastructures. Civil Engineering Journal 8, 24–32. https://doi.org/10.28991/CEJ-2022-08-01-02.

Rusu, L., 2022. The near future expected wave power in the coastal environment of the Iberian Peninsula. Renew. Energy 195, 657–669. https://doi.org/10.1016/J.RENENE.2022.06.047.

Rusu, L., 2020. A projection of the expected wave power in the Black Sea until the end of the 21st century. Renew. Energy 160, 136–147. https://doi.org/10.1016/J.RENENE.2020.06.092.

Rusu, L., 2019a. Evaluation of the near future wave energy resources in the Black Sea under two climate scenarios. Renew. Energy 142, 137–146. https://doi.org/10.1016/J.RENENE.2019.04.092.

Rusu, L., 2019b. The wave and wind power potential in the western Black Sea. Renew. Energy 139, 1146–1158. https://doi.org/10.1016/J.RENENE.2019.03.017.

Rusu, L., GuedesSoares, C., 2014. Local data assimilation scheme for wave predictions close to the Portuguese ports. Journal of Operational Oceanography 7, 45–57. https://doi.org/10.1080/1755876X.2014.11020158.

Shimura, T., Mori, N., Mase, H., 2015. Future projection of ocean wave climate: analysis of SST impacts on wave climate changes in the western North pacific. J. Clim. 28, 3171–3190. https://doi.org/10.1175/JCLI-D-14-00187.1.

Sierra, J.P., Casas-Prat, M., Campins, E., 2017. Impact of climate change on wave energy resource: the case of Menorca (Spain). Renew. Energy 101, 275–285. https://doi.org/10.1016/J.RENENE.2016.08.060.

Silva, D., Bento, A.R., Martinho, P., Soares, G., 2015. High Resolution Local Wave Energy Modelling in the Iberian Peninsula. https://doi.org/10.1016/j.energy.2015.08.067.

Silva, D., Martinho, P., Guedes Soares, C., 2018. Wave energy distribution along the Portuguese continental coast based on a thirty three years hindcast. Renew. Energy 127, 1064–1075. https://doi.org/10.1016/J.RENENE.2018.05.037.

SWAN Team, 2020. SWAN User Manual—SWAN Cycle III Version 41.45 A. Delft University of Technology, p. 2600.

Tabari, H., 2020. Climate change impact on flood and extreme precipitation increases with water availability. Scientific Reports 2020 10 (1 10), 1–10. https://doi.org/10.1038/s41598-020-70816-2.

Taylor, K.E., Stouffer, R.J., Meehl, G.A., 2012. An overview of CMIP5 and the experiment design. Bull. Am. Meteorol. Soc. 93, 485–498. https://doi.org/10.1175/BAMS-D-11-00094.1.

The European Green Deal, 2020. URL. https://commission.europa.eu/strategy-andpolicy/priorities-2019-2024/european-green-deal_en. (Accessed 17 February 2023).

Weatherall, P., Marks, K.M., Jakobsson, M., Schmitt, T., Tani, S., Arndt, J.E., Rovere, M., Chayes, D., Ferrini, V., Wigley, R., 2015. A new digital bathymetric model of the

world's oceans. Earth Space Sci. 2, 331–345. https://doi.org/10.1002/2015EA000107.

Yukimoto, S., Adachi, Y., Hosaka, M., Sakami, T., Yoshimura, H., Hirabara, M., Tanaka, T.Y., Shindo, E., Tsujino, H., Deushi, M., Mizuta, R., Yabu, S., Obata, A., Nakano, H., Koshiro, T., Ose, T., Kitoh, A., 2012. A new global climate model of the meteorological research institute: MRI-CGCM3 —model description and basic performance. Journal of the Meteorological Society of Japan. Ser. II 90A 23–64. https://doi.org/10.2151/JMSJ.2012-A02.

Zijlema, M., 2010. Computation of wind-wave spectra in coastal waters with SWAN on unstructured grids. Coast. Eng. 57, 267–277. https://doi.org/10.1016/j.coastaleng.2009.10.011.